THE JOURNAL OF BIOLOGICAL CHEMISTRY VOL. 283, NO. 26, pp. 18355–18364, June 27, 2008

Unique Asn-linked Oligosaccharides of the Human Pathogen *Entamoeba histolytica*[*] [S]

Received for publication, January 28, 2008, and in revised form, March 21, 2008 Published, JBC Papers in Press, April 16, 2008, DOI 10.1074/jbc.M800725200

Paula Magnelli[‡], John F. Cipollo[§], Daniel M. Ratner[‡], Jike Cui[‡], Daniel Kelleher[¶], Reid Gilmore[¶], Catherine E. Costello[§], Phillips W. Robbins[‡], and John Samuelson[‡1]

From the [‡]Department of Molecular and Cell Biology and the [§]Mass Spectrometry Resource, Department of Biochemistry, Boston University Medical Center, Boston, Massachusetts 02118-2526 and the [¶]Department of Biochemistry and Molecular Pharmacology, University of Massachusetts Medical School, Worcester, Massachusetts 01605-2324

***N*-Glycans of *Entamoeba histolytica*, the protist that causes amebic dysentery and liver abscess, are of great interest for multiple reasons. *E. histolytica* makes an unusual truncated *N*-glycan precursor ($Man_5GlcNAc_2$), has few nucleotide sugar transporters, and has a surface that is capped by the lectin concanavalin A. Here, biochemical and mass spectrometric methods were used to examine *N*-glycan biosynthesis and the final *N*-glycans of *E. histolytica* with the following conclusions. Unprocessed $Man_5GlcNAc_2$, which is the most abundant *E. histolytica N*-glycan, is aggregated into caps on the surface of *E. histolytica* by the *N*-glycan-specific, anti-retroviral lectin cyanovirin-N. $Glc_1Man_5GlcNAc_2$, which is made by a UDP-Glc:glycoprotein glucosyltransferase that is part of a conserved *N*-glycan-dependent endoplasmic reticulum quality control system for protein folding, is also present in mature *N*-glycans. A swainsonine-sensitive α-mannosidase trims some *N*-glycans to biantennary $Man_3GlcNAc_2$. Complex *N*-glycans of *E. histolytica* are made by the addition of α1,2-linked Gal to both arms of small oligomannose glycans, and Gal residues are capped by one or more Glc. In summary, *E. histolytica N*-glycans include unprocessed $Man_5GlcNAc_2$, which is a target for cyanovirin-N, as well as unique, complex *N*-glycans containing Gal and Glc.**

Entamoeba histolytica is the protist (single cell eukaryote) that causes millions of cases of amebic dysentery and liver abscess in regions where its fecal-oral spread cannot be prevented (1, 2). Asn-linked glycans (*N*-glycans) of *E. histolytica* are of great interest for seven reasons.

First, *E. histolytica* is missing many of the glycosyltransferases that make lipid-linked precursors to *N*-glycans and so makes a $Man_5GlcNAc_2$-PP-dolichol rather than $Glc_3Man_9GlcNAc_2$-PP-dolichol, which is present in most animals, plants, and fungi (3, 4). Second, *E. histolytica N*-glycans contribute to the quality control of protein folding in the endoplasmic reticulum (ER)[2] (4–6). In particular, *E. histolytica* has UDP-Glc:glycoprotein glucosyltransferase, calreticulin, glucosidase II, and ERGIC-53, which are the essential components of an *N*-glycan-dependent quality control system (4–6).

Third, the *E. histolytica* oligosaccharyltransferase (OST), which transfers *N*-glycans from the dolichol pyrophosphate-linked precursor to Asn on the nascent peptide in the lumen of the ER is composed of four subunits rather than seven or eight subunits found in metazoan, fungi, and plants (7). As a result, the *E. histolytica* OST has different kinetics than the OSTs of higher eukaryotes (8). As well, the *E. histolytica* OST prefers to transfer *N*-glycans, which resemble its own ($Man_5GlcNAc_2$), rather than the longer *N*-glycans of metazoa and fungi ($Glc_3Man_9GlcNAc_2$) (8).

Fourth, *E. histolytica* has a limited set of nucleotide sugar transporters (UDP-Gal and UDP-Glc), which transport activated sugars into the lumen of the ER and Golgi (9). UDP-Gal and UDP-Glc are used to make unique *O*-phosphodiester-linked glycans of *E. histolytica* proteophosphoglycans (10) and may be used to make complex *N*-glycans.

Fifth, *E. histolytica* causes disease when the protist uses a Gal- and GalNAc-binding lectin on its surface to adhere to mucins on the surface of host colonic epithelial cells and then lyses host cells by means of secreted proteases and pore-forming peptides (1, 2, 11, 12). Heavy subunits of the *E. histolytica* Gal/GalNAc lectins have 7–14 potential sites for *N*-linked glycosylation, and inhibition of *N*-glycan synthesis results in a Gal/GalNAc lectin that is unable to bind its target (11).

Sixth, the plant lectin concanavalin A binds to glycoproteins on the surface of *E. histolytica* and aggregates them into caps that are shed into the medium (13). This result suggests the possibility that *E. histolytica* may have on its surface high mannose *N*-glycans. In a similar way, gp120 of HIV has on its surface *N*-glycans composed of $Man_9GlcNAc_2$ (14). These high mannose *N*-glycans on gp120 are the target of an anti-HIV human monoclonal antibody (2G12) and of bacterial anti-retroviral lectins (cyanovirin-N and scytovirin) (15, 16).

* This work was supported, in whole or in part, by National Institutes of Health Grants AI 44070 (to J. S.), GM 43768 (to R. G.), P41 RR10888 and S10 RR15942 (to C. E. C.), and GM 31318 (to P. W. R.). The costs of publication of this article were defrayed in part by the payment of page charges. This article must therefore be hereby marked "*advertisement*" in accordance with 18 U.S.C. Section 1734 solely to indicate this fact.

[S] The on-line version of this article (available at http://www.jbc.org) contains supplemental Table 1, Figs. 1–5, and additional references.

[1] To whom correspondence should be addressed: Dept. of Molecular and Cell Biology, Boston University Goldman School of Dental Medicine, 715 Albany St., Evans 426, Boston, MA 02118. Tel.: 617-414-1054; Fax: 617-414-1041; E-mail: jsamuels@bu.edu.

[2] The abbreviations used are: ER, endoplasmic reticulum; MS, mass spectrometry; HPAEC, high performance anion exchange chromatography; PBS, phosphate-buffered saline; TPCK, L-1-tosylamido-2-phenylethyl chloromethyl ketone; MES, 4-morpholineethanesulfonic acid; MALDI-TOF, matrix-assisted laser desorption ionization time-of-flight; Hex_n, $Hex_nGlcNAc_2$; NYT, N^{α}-acetyl-*N*-^{125}I-Tyr-Thr-NH_2; OST, oligosaccharyltransferase; PNGase F, peptide:*N*-glycanase F; HPLC, high pressure liquid chromatography.

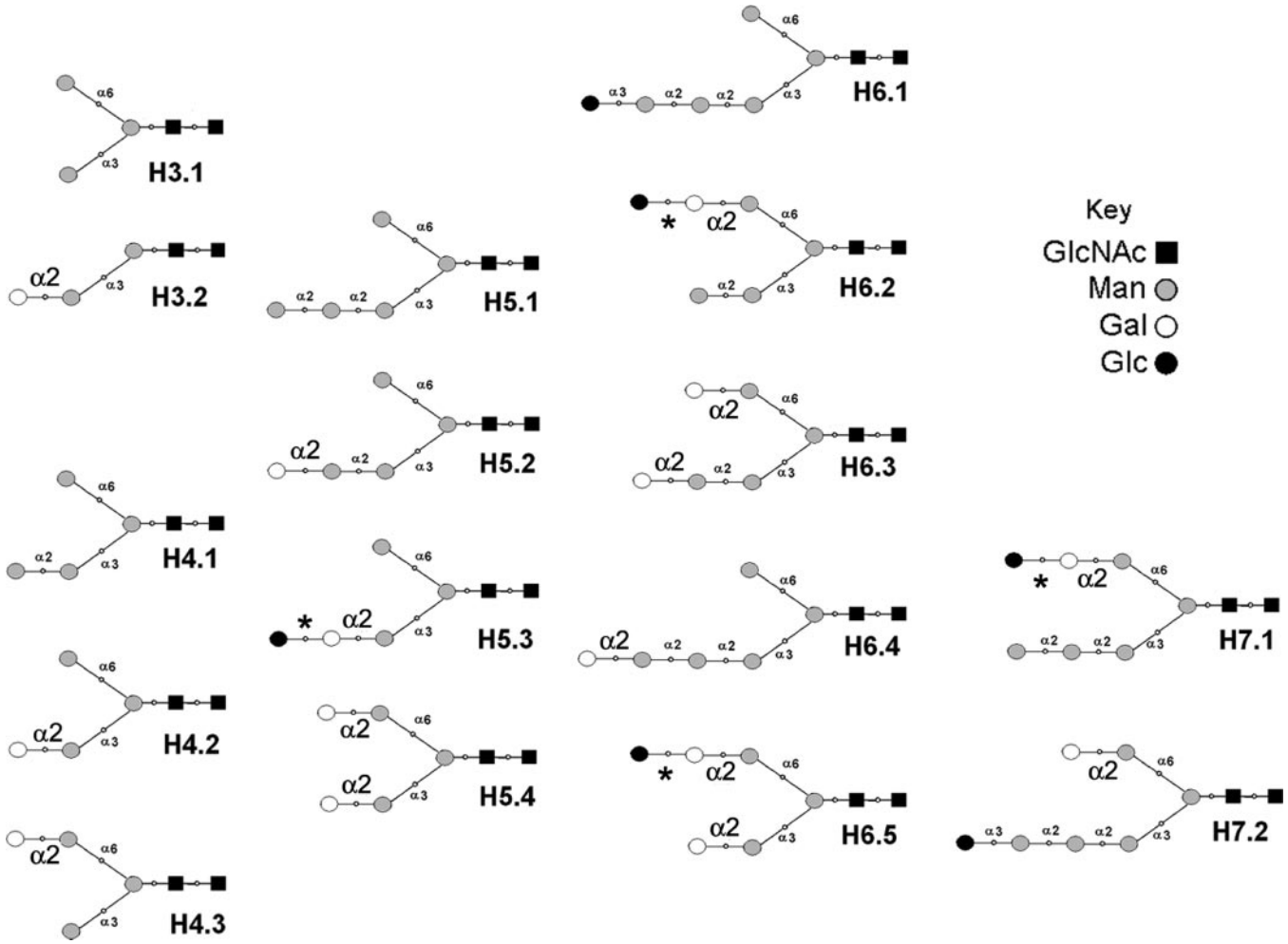

FIGURE 1. ***E. histolytica*** **trophozoites make numerous *N*-glycans from the truncated $Man_5GlcNAc_2$ precursor transferred by the OST (3, 8).** The most abundant *N*-glycan in each size range is listed first (*e.g.* H3.1, H4.1, etc.). Structures were identified by multiple techniques including *in vivo* and *in vitro* labeling, size separation on Bio-Gel P-4 and HPAEC, glycosylhydrolase digestions, monosaccharide analysis, and mass spectrometry. An *asterisk* marks the linkage between Glc and Gal, which could not be determined experimentally.

Seventh, although *N*-linked glycans of *Giardia lamblia* and kinetoplastids (*e.g. Trypanosoma cruzi*, *Trypanosoma brucei*, and *Leishmania mexicana*) have been characterized, *N*-glycans of the vast majority of protists (*e.g. E. histolytica*, *Trichomonas vaginalis*, *Plasmodium falciparum*, *Toxoplasma gondii*, and *Cryptosporidium parvum*) remain uncharacterized (3, 17–19). Characterization of *E. histolytica N*-glycans then may lead to a better understanding of the diversity of *N*-linked glycosylation in protists and may identify novel sugar linkages that have not previously been identified in higher eukaryotes.

Here, biochemical methods including *in vivo* and *in vitro* labeling, as well as mass spectrometry, were used to characterize *E. histolytica N*-glycans. *E. histolytica N*-glycans include unprocessed $Man_5GlcNAc_2$, which is a target for cyanovirin-N, as well as unique, complex *N*-glycans containing Gal and Glc.

EXPERIMENTAL PROCEDURES

Bioinformatic Predictions—The predicted proteins of the *E. histolytica* genome, which has been extensively sequenced, were searched with BLASTP and representatives (*e.g. Saccharomyces*, *Homo*, or *Escherichia*) of each of 79 glycosyltransferase families and 104 glycosylhydrolase families present in the data base of carbohydrate-active enzymes (CAZy) (20–22). Putative *E. histolytica* glycosyltransferases and glycosylhydrolases were compared with proteins in the NR Database and to the conserved domain data base at the NCBI using PSI-BLAST. Signal peptides and transmembrane helices of *E. histolytica* proteins were predicted using SignalP and TMHMM, respectively (23, 24).

Reagents—[2-^{3}H]Man (30 Ci/mmol), [U-^{14}C]Glc (200 mCi/mmol), UDP-[^{3}H]Gal (5.8 Ci/mmol), and UDP-[^{3}H]Glc (300 mCi/mmol) were from American Radiolabeled Chemicals (St. Louis, MO). Peptide:*N*-glycanase F (PNGase F) was from New England Biolabs. Jack bean α-mannosidase and almond β-glucosidase were from Sigma. Coffee bean α-galactosidase, β1,3,4,6-galactosidase, and β-glycosidase II (β-galactosidase and β-glucosidase activities) were from Calbiochem. *Aspergillus saitoi* α1,2-mannosidase, bovine testes β-galactosidase, Jack bean hexosaminidase, $Man_3GlcNAc_2$, and $Man_1GlcNAc_2$ standards were from Glyko (San Leandro, CA). Maltase and amyloglucosidase (α-glucosidases) were from Roche Applied Science. Golgi endomannosidase (25) was a generous gift from Dr. Robert Spiro (Harvard Medical School). Cyanovirin-*N* and

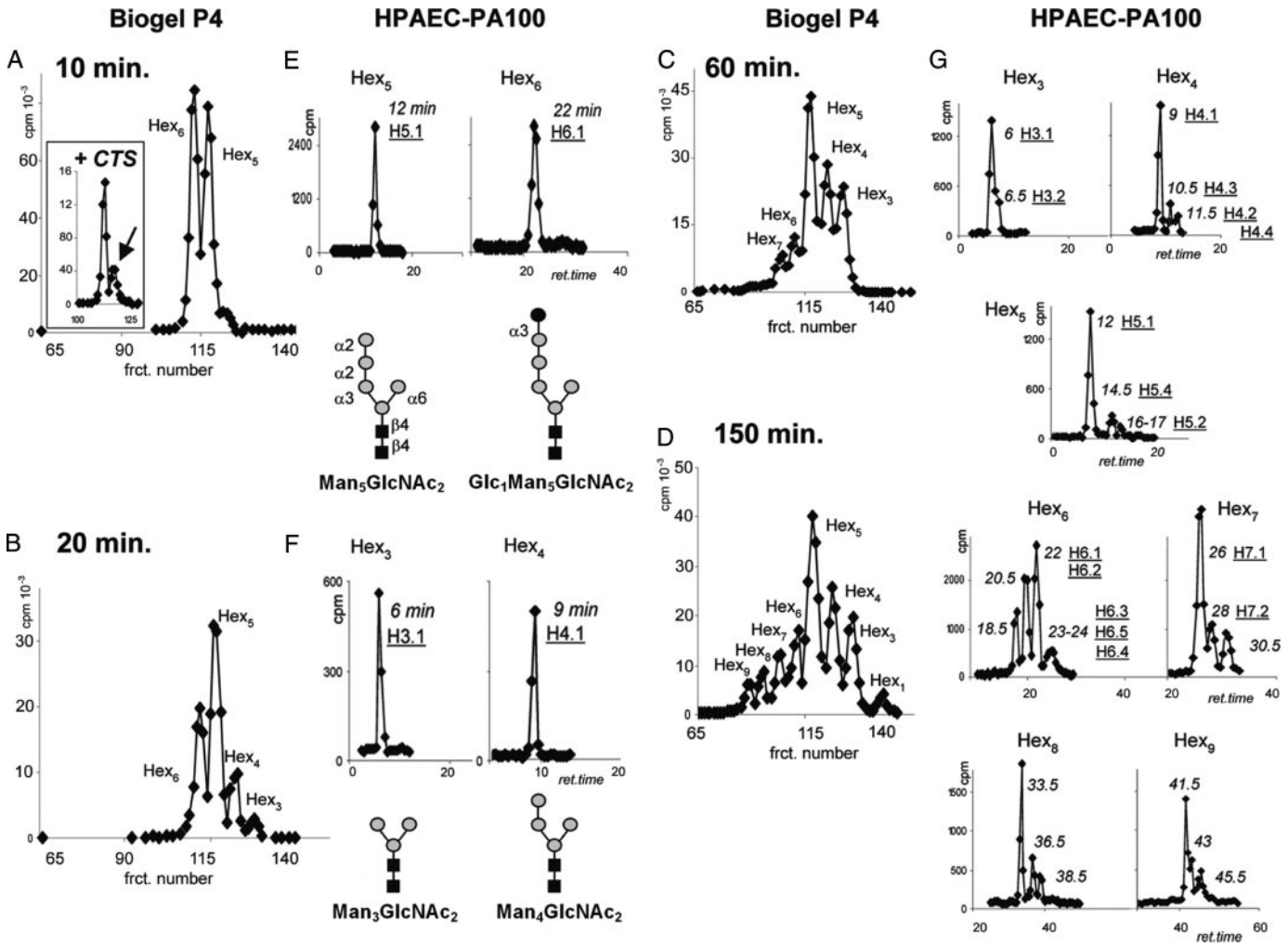

FIGURE 2. **The complexity of *N*-glycans made by *E. histolytica* trophozoites increases dramatically with time.** *E. histolytica* trophozoites were incubated with [2-^{3}H]Man for 10, 20, 60, and 150 min, and *N*-glycans were released with PNGase F and separated by Bio-Gel P-4 filtration (*A–D*), where Hex_n indicates their size. Isomers with the same number of hexoses were further isolated on an HPAEC-PA100 column (*E–H*), with the retention time (*ret.*; min) shown in *italic* and the identifier name from Fig. 1 (*e.g.* H5.1) *underlined* below. After 10-min labeling (*A* and *E*), the predominant *E. histolytica* *N*-glycans were unmodified $Man_5GlcNAc_2$ and the glucosylated product of UDP-Glc:glycoprotein glucosyltransferase ($Glc_1Man_5GlcNAc_2$) (H6.1). As shown in the *inset* in *A*, $Glc_1Man_5GlcNAc_2$ is by far the most abundant *N*-glycan in the presence of the glucosidase II inhibitor castanospermine (*CTS*). After 20-min labeling (*B* and *F*), two mannosidase digestion products are apparent: $Man_4GlcNAc_2$ (H4.1) and $Man_3GlcNAc_2$ (H3.1). After 60-min labeling (*C*), complex *N*-glycans are apparent in Hex_6 and Hex_7 pools. After 150-min labeling (*D* and *G*), novel, complex *N*-glycans are present in all of the pools (see further characterization in Fig. 4). *frct.*, fraction.

scytovirin were generous gifts of Barry O'Keefe (NCI-Frederick, National Institutes of Health).

In Vivo Labeling Conditions—E. histolytica strain HM1:IMSS was grown axenically in TYI-S-33 medium containing 0.1% (w/v) Glc to minimize the storage of glycogen, in which fragments otherwise contaminate *N*-glycan extracts (26). *E. histolytica* cultures from five 32 cm^2 flasks were combined, centrifuged, and transferred to a microcentrifuge tube with 0.5 ml of radiolabeling medium (the same as described above, excluding Glc and containing 200 μCi of [2-^{3}H]Man or 2 mCi of [^{14}C]Glc) (3). Amebas were incubated for the indicated time at 37 °C and then washed in PBS several times before processing.

Extraction of N-Glycans—Non-incorporated radiolabel was removed by washing the cell pellet with 50% methanol. Cells were lysed with a Dounce homogenizer in 4 ml of Tris-HCl buffer, pH 8. To reprecipitate proteins, the pH was adjusted to 5 with acetic acid, and 4 ml of methanol was added. Tubes were chilled at −20 °C for 4 h and centrifuged at 14,000 rpm for 10 min. This step was repeated twice to wash out soluble glycans such as glycogen fragments. The methanol-denaturated protein pellet was dispersed and treated with 5,000 units of PNGase F in acetate buffer, pH 5, at 37 °C for 16 h. The suspension containing the released *N*-glycans in solution was adjusted to 50% methanol to precipitate large carbohydrates and proteins. After 4 h at −20 °C, the supernatant was cleared by centrifugation and dried. Oligosaccharides were further purified on a porous graphitic carbon Hypercarb column (Thermo Keystone) and washed with 3 ml of distilled water. The *N*-glycans, which were eluted with 30% acetonitrile, 0.1% trifluoroacetic acid, were dried and resuspended in 300 μl of water.

In Vitro Labeling of N-Glycans—Intact *E. histolytica* vesicles from freshly harvested cultures were prepared as described for nucleotide sugar transport assays (9), excluding separation ER enriched vesicles from light Golgi enriched vesicles. Labeling of endogenous acceptors was performed by incubating the *E. histolytica* vesicles with UDP-[^{3}H]Gal and UDP-[^{14}C]Glc as

described (9). The vesicle preparation still carried a significant amount of cytosolic epimerase activity, which converts UDP-Gal to UDP-Glc, in a reversible reaction. Because of this activity, [^{3}H]Glc was incorporated into *E. histolytica* glycoproteins when labeling with UDP-[^{3}H]Gal and vice-versa. Therefore, specific labeling was not possible. The labeling of glycans was started by mixing 500 μl of vesicle suspension and 500 μl of reaction buffer (10 mM $MnCl_2$, 10 mM $MgCl_2$, 10 mM $CaCl_2$, 0.5 M sucrose, 30 mM triethanolamine, pH 7.2, 5 μM UDP-Gal, and 5 μM UDP-Glc and 30 μCi of each radiolabeled precursor). After 45 min at 37 °C, the reaction was diluted with 1 volume of 100 μM UDP-Gal and UDP-Glc and separated into 100-μl aliquots, each of which was precipitated with 900 μl of 4% perchloric acid. After chilling on ice for 30 min, the preparation was centrifuged at 16,000 $\times$ *g* for 30 min, and the pellets were combined and neutralized. The pellets were resuspended with 2 ml of 10 mM Tris-HCl buffer, pH 8, in 50% methanol and homogenized in a 3-ml Dounce. After 2 h at −4 °C, the suspension was centrifuged at 14,000 $\times$ *g* for 10 min, and the pellet was washed twice with Tris-HCl buffer, pH 8, to remove traces of methanol prior to release of *N*-glycans by digestion with PNGase F (see conditions above).

Sample Preparation for Mass Spectrometry—The starting material to isolate *N*-glycans for mass spectrometry was a cell pellet obtained from 60 flasks of *E. histolytica* culture. First, lipids were extracted three times with 30 ml of chloroform: methanol (1:1) and three times with 30 ml of chloroform:methanol:water (10:10:3). Soluble carbohydrates (mostly glycogen fragments) were removed by extracting three times with 20 ml of 10 mM Tris-HCl buffer, pH 8, and reprecipitating with 1 volume of chilled methanol for 4 h at −20 °C. After a final wash in buffer, the pellet was digested with 1 μg of TPCK-treated trypsin in 1 ml of 10 mM Tris-HCl buffer, pH 8, for 16 h at 37 °C. After boiling to inactivate the protease, the suspension was digested with 20 $\times$ 10^3 units of PNGase F in the presence of phenylmethylsulfonyl fluoride for 16 h at 37 °C. The mixture was precipitated with 50% methanol, and the supernatant was purified through a porous graphite column, followed by passage through a 3-ml Amberlite mixed bed ion exchange column (H^+/acetate form). Finally, the *N*-glycan extract was dried and resuspended in 300 μl of water.

Chromatography—A Bio-Gel P-4 superfine mesh column of 1 $\times$ 120 cm was equilibrated in 0.1 M acetic acid, 1% *n*-butyl alcohol. 300 μl of glycan sample was applied and run at a constant flow rate of 5 ml/h, and 1.3-ml fractions were collected. Radioactivity was determined by liquid scintillation counting. The distribution coefficient (K_d = (Ve − Vo)/(Vt − Vo)) was determined using the glycan elution volume (Ve) relative to the elution of cytochrome C (marker for the exclusion volume; Vo) and glucose (marker for the total volume; Vt). GlcNAc, diacetylchitobiose, and radiolabeled $Man_5GlcNAc_2$ (prepared from the dolichol-linked precursors of Δ*alg3 Saccharomyces cerevisiae* (4)) were used to calibrate the system. For non-radiolabeled samples, peaks were collected according to the K_d of equivalent radiolabeled specimens.

To separate isomers with the same molecular mass, fractions obtained by gel filtration were separated by high performance anion exchange chromatography (HPAEC) with a pulse amperometric detector in a Dionex LC20 instrument through a PA100 column (250 $\times$ 4 mm) equilibrated in 150 mM NaOH. The flow rate was 0.6 ml/min with a sodium acetate gradient from 12.5 mM (0–3 min) to 50 mM (at 31 min) and finally to 175 mM (at 70 min). A desalter membrane was installed to remove sodium ions, neutralizing the carbohydrate-containing eluent. Fractions of 0.3 ml were collected, and aliquots were taken for scintillation counting. The retention time of each isomer was determined. The system was calibrated with known *N*-glycans ($Man_3GlcNAc_2$, $Man_1GlcNAc_2$, and $Man_5GlcNAc_2$ prepared from Δ*alg3 S. cerevisiae* cells) and with the series laminaribiose, laminaritriose, and laminaritetraose (routinely used as internal markers). Non-radiolabeled samples for mass spectrometry were isolated on a 250 $\times$ 9 mm semi-preparative PA100 column (flow rate of 1.5 ml/min, collecting 0.7-ml fractions) calibrated and operated (excluding the internal markers) as described above. Carbohydrate-containing peaks were detected by a pulse amperometric detector, and the corresponding fractions were pooled and dried.

Ion Exchange Mini-columns—The resins used were Dowex 50 (H+ form), Dowex 1 (formate form), and Amberlite mixed bed (IRA-400 H+ form and IR-120 acetate form). Columns (0.5 $\times$ 2.5 cm) were equilibrated in deionized water. The glycan sample (0.5 ml) was applied followed by water washes, and fractions of 0.25 ml were collected for scintillation counting. The retention behavior of glycans was compared with neutral or charged standards ([2-^{3}H]Man, [^{3}H]GlcN, [^{3}H]Glc 1-phosphate, and UDP-[^{3}H]Glc).

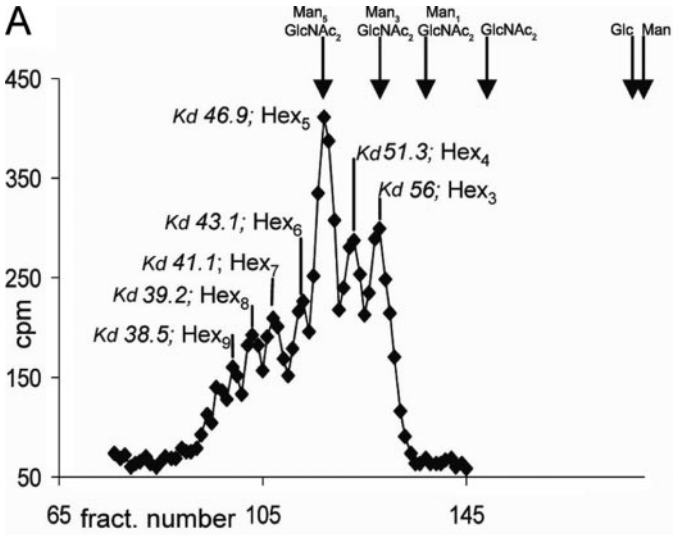

B

	Hex_3	Hex_4	Hex_5	Hex_6	Hex_7	$Hex_{8/9}$
mannose	99.3	89.3	94.0	74.6	75.9	71.8
glucose	0.0	3.5	3.6	18.5	19.1	23.5
galactose	0.7	7.2	2.5	6.9	5.0	4.7

FIGURE 3. **The abundance of Glc in complex *N*-glycans of *E. histolytica* trophozoites increases with their length.** *A*, *E. histolytica* *N*-glycans labeled with [U-^{14}C]Glc and separated by Bio-Gel P-4 filtration. The number of hexoses in each glycomer is indicated (Hex_n), according to calibrated standards prepared from $Man_5GlcNAc_2$ digested with jack bean α-mannosidase and *A. saitoi* α1,2-mannosidase. *B*, relative abundance (weight percentage) of neutral sugars for each peak after acid hydrolysis, as determined by HPAEC chromatography. *fract.*, fraction.

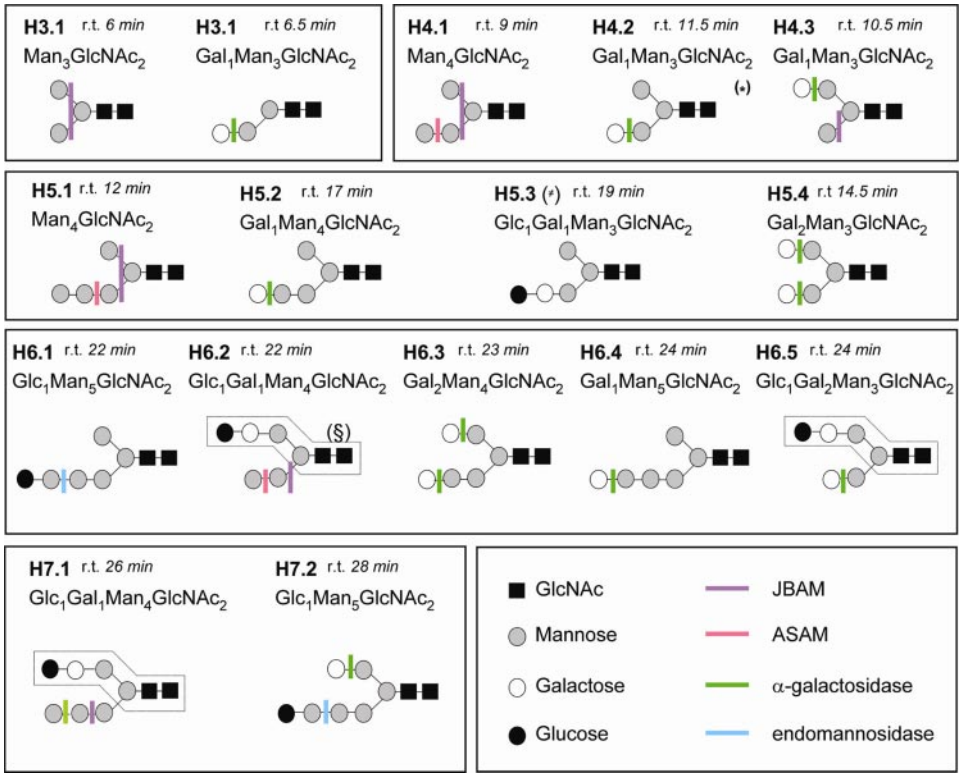

FIGURE 4. **Characterization of the *E. histolytica* *N*-glycans by *in vivo* labeling and glycosylhydrolase digestions.** *E. histolytica* *N*-glycans, which were prepared as in Fig. 2, were treated with glycosylhydrolases, and digestion products were identified according to retention times (*r.t.*) of known standards (*e.g.* $Man_3GlcNAc_2$). For isomers H6.2, H6.5, and H7.1, the *dashed line* enclosing the Manα1,6- arm indicates what corresponds to the residual fragment 11.5, which was fully characterized in a separate [U-^{14}C]Glc-labeling experiment. Note that jack bean α-mannosidase (*JBAM*) removes an exposed Manα1,3- (as in isomer H4.3), but it does not remove the Manα1,6- unless the Manα1,3- arm is digested first. Hence, isomer H4.2 becomes susceptible to jack bean α-mannosidase digestion only after removal of Galα1,2- by α-galactosidase. The mode of action of jack bean α-mannosidase (37) supports our assumption that the different sensitivities of H4.2 and H4.3 are due to accessibility of α-linked Man residues. In accordance with this, the underlying structures of other isomers were inferred as well. *ASAM*, *A. saitoi* α1,2-mannosidase.

Glycosylhydrolase Digestions—All the glycosylhydrolase digestions were performed in a volume of 100 μl for 16 h at 37 °C. The conditions were adjusted by digestion of known glycans to assure a complete reaction. A final concentration of 100 mM potassium phosphate buffer, pH 6.5, was used for coffee bean α-galactosidase, maltase, and amyloglucosidase; 100 mM sodium acetate buffer, pH 4.8, was used for Jack bean α-mannosidase, β-glucosidase, β1,3,4,6-galactosidase, α1,2-mannosidase, β-glycosidase II, bovine testes β-galactosidase, and Jack bean hexosaminidase digestions. A Golgi endomannosidase reaction was performed in 100 mM Na-MES buffer, pH 6.5, supplemented with 0.1% Triton X-100 and 50 μg/ml bovine serum albumin.

Monosaccharide Composition—Radiolabeled samples were dried, resuspended in 300 μl of 2 N HCl in microcentrifuge tubes flushed with N_2 to minimize oxidation, and hydrolyzed for 2 h at 90 °C. Acid was removed by several rounds of evaporation under N_2. The neutral sugars were separated by HPAEC on a MA1 250 × 4 mm column (flow rate of 0.4 ml/min, collecting 0.2-ml fractions) with an NaOH gradient from 100 mM (0–3 min) to 850 mM (to 45 min). GlcN, Glc, Man, and Gal were used as internal standards.

Mass Spectrometry—Oligosaccharides were permethylated as described previously (27). MALDI-TOF MS was performed on a Bruker Reflex IV mass spectrometer in positive reflectron mode. Between 20 and 50 pmol of sample dissolved in 20% acetonitrile was applied to the MALDI target with an equal volume of 2,5-dihydroxybenzoic acid (20 mg/ml) in 20% acetonitrile with 10 mM sodium acetate added as a cation source. The spectra resulting from 150 and 200 shots from a 337-nm nitrogen laser were summed. The laser pulse was 3 ns. Collision-induced dissociation fragmentation data were collected using a QStar Pulsar i quadruple orthogonal time-of-flight mass spectrometer (Applied Biosystems Inc., Framingham, MA) equipped with an electrospray ionization source. Capillaries were pulled to a 1-micron orifice diameter. Argon (3 p.s.i.) was used as the collision gas for MS/MS experiments. The range of operator-controlled collision voltages was 35–90 V. Between 2 and 3 pmol of sample were consumed during each MS/MS experiment. The mass spectrometer parameters were as follows for MS/MS experiments: DP1, 75.0 V; FP, 245.0 V; DP2, 30.0 V; CG, 3.0 p.s.i.; IRD, 6.0 V; IRW, 5.0 V; GS1, 5.0 p.s.i.; GS2, 10.0 p.s.i.; and CUR, 12.0 p.s.i. The ion spray voltage was between 4,000 and 4,500 V. For pseudo MS/MS/MS experiments, the following parameters were used: DP1, 130.0 V; FP, 300.0 V; DP2, 40.0 V; CG, 3.0 p.s.i.; IRD, 6.0 V; IRW, 5.0 V; GS1, 5.0 p.s.i.; GS2, 10.0 p.s.i.; and CUR, 12.0 V. Nomenclature is that of Domon and Costello (28) unless otherwise indicated.

In Vitro OST Assay—Total cellular membranes of *E. histolytica* were incubated for 2–90 min at 37 °C with the membrane-permeable tripeptide acceptor 5 μM N^{α}-acetyl-*N*-^{125}I-Tyr-Thr-NH_2 (NYT) in the presence of deoxynojirimycin to ensure that the glycopeptide products were not degraded by glucosidases I and II (29, 30). In some experiments, swainsonine was added to determine the effect of endogenous *E. histolytica* mannosidases on glycopeptides. Glycopeptide products were collected by binding to immobilized concanavalin A and separated by HPLC using an aminopropyl silica column. Glycopeptide standards ($Man_5GlcNAc_2$-NYT and $Man_9GlcNAc_2$-NYT) were prepared using the *Saccharomyces* OST and purified dolichol-linked oligosaccharides (31).

Cyanovirin-N Labeling and Capping of E. histolytica—Freshly harvested *E. histolytica* were washed three times with PBS and incubated with 20 μg/ml BODIPY-labeled cyanovirin-N for 30 min at 4 °C (14, 15). Unbound cyanovirin-N was removed by rinsing twice with PBS. For surface labeling, *E. his-*

tolytica were immediately fixed with 2% paraformaldehyde in PBS for 10 min at 4 °C. To determine whether cyanovirin-N aggregates and forms caps on the surface of *E. histolytica*, we incubated cyanovirin-N-bound cells in PBS for 15 min at 37 °C and subsequently fixed them in 2% paraformaldehyde. For labeling the internal membranes and surface of *E. histolytica*, amebas were fixed in 2% paraformaldehyde and 0.1% Triton X-100. Organisms were visualized with a DeltaVision deconvoluting microscope (Applied Precision, Issaquah, WA) with the help of Landon Moore of the Department of Genetics and Genomics at Boston University School of Medicine. Images were taken at ×100 primary magnification and deconvolved using Applied Precision softWoRx software.

RESULTS

Brief Summary of the Experimental Strategy—The structures of *E. histolytica N*-glycans, which are shown in Fig. 1, were determined by *in vivo* labeling with [2-^{3}H]Man (shown in Fig. 2) or [U-^{14}C]Glc (shown in Fig. 3) or by the separation of *N*-glycans released by PNGase F on Bio-Gel P-4 and HPAEC, followed by digestion with specific glycosylhydrolases (shown in Fig. 4). Alternatively, *E. histolytica N*-glycans were identified by *in vitro* labeling of *E. histolytica* membranes with nucleotide sugars (nucleotide sugar transfer assays shown in Fig. 6) or with a radiolabeled tripeptide (OST assays shown in Fig. 7). In addition, *E. histolytica N*-glycans were examined by mass spectrometry (shown in Figs. 8 and 9). These strategies allowed us to identify each *E. histolytica N*-glycan by multiple methods. Finally, we localized unprocessed *N*-glycans on the surface of *E. histolytica* using the anti-retroviral lectin cyanovirin-N (shown in Fig. 5).

The Most Abundant N-Glycan of E. histolytica Is Unprocessed Biosynthetic $Man_5GlcNAc_2$—The most abundant *N*-glycan of *E. histolytica* after *in vivo* labeling for 20–150 min with [^{3}H]Man or for 3 h with [^{14}C]Glc (Figs. 2 and 3) was unprocessed, biosynthetic $Man_5GlcNAc_2$ (H5.1 in Fig. 1), which was characterized by mannosidase digestions (Fig. 4). When *E. histolytica* were pulse-labeled for 10 min with [2-^{3}H]Man, washed, and chased for 3 h with unlabeled Man, biosynthetic $Man_5GlcNAc_2$ was still the most abundant *N*-glycan (data not shown). This result shows that many *E. histolytica N*-glycoproteins are not modified by Golgi-type glycosylhydrolases and glycosyltransferases.

$Man_5GlcNAc_2$ on the Surface of E. histolytica Trophozoites Is Bound and Capped by the Anti-retroviral Lectin Cyanovirin-N—The presence of biosynthetic $Man_5GlcNAc_2$ (H5.1) on the surface of cultured *E. histolytica* was demonstrated using the anti-retroviral lectin cyanovirin-N (Fig. 5) (15). Cyanovirin-N is specific for the Manα1,2-Man- on the single D1 arm of $Man_5GlcNAc_2$ (*E. histolytica N*-glycans) or on three arms of $Man_9GlcNAc_2$ (*N*-glycans of gp120) (Fig. 5*A*). Cyanovirin-N was bound to the surface and vesicular membranes of fixed and permeabilized *E. histolytica* (Fig. 5*B*). Cyanovirin-N was also bound evenly to glycoproteins on the surface of chilled but living *E. histolytica* (Fig. 5*C*). When *E. histolytica* were warmed to 37 °C, cyanovirin-N aggregated into caps (Fig. 5*D*), which resemble those formed by the lectin concanavalin A on the *E. histolytica* surface (11, 13). As a negative control, scytovirin, another anti-retroviral lectin that is specific for Man on the upper (D3) arm of $Man_9GlcNAc_2$, which is absent from *E. histolytica N*-glycans, did not bind to the surface or vesicles of *E. histolytica* (data not shown) (15).

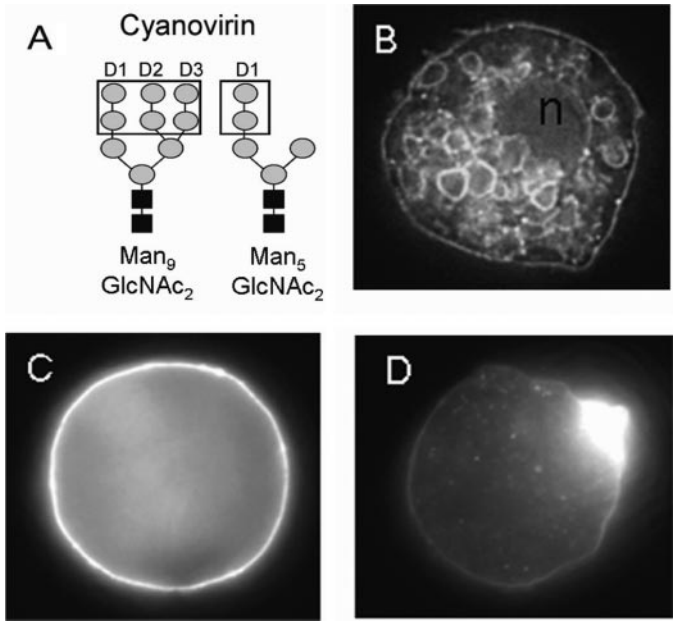

FIGURE 5. **The anti-retroviral lectin cyanovirin-N, which recognizes high Man *N*-glycans (15, 16), binds to the surface *E. histolytica* trophozoites and forms caps.** *A*, cyanovirin-N binds to terminal α1,2-linked Man, which is present on each of the three arms of $Man_9GlcNAc_2$ and is also present on the single arm of $Man_5GlcNAc_2$. *B*, cyanovirin-N binds to the surface and to vesicular membranes of fixed and permeabilized *E. histolytica*. *n*, nucleus. *C*, cyanovirin-N is evenly distributed on the surface of a live *E. histolytica* incubated with the lectin in the cold, so it cannot cap. *D*, cyanovirin-N is capped on the surface of a live *E. histolytica* that is allowed to warm up to 37 °C for 10 min. The negative control was scytovirin (a lectin that binds to an intact D3 arm, which is absent in *E. histolytica N*-glycans). *E. histolytica* incubated with scytovirin were not labeled (data not shown).

$GlcMan_5GlcNAc_2$, the Product of UDP-Glc:Glycoprotein Glucosyltransferase Involved in N-Glycan-dependent Quality Control of Protein Folding, Is Also Present in Mature N-Glycans of E. histolytica—At the earliest time points of metabolic labeling with [2-^{3}H]Man (Fig. 2*A*), *E. histolytica N*-glycans were composed of $Man_5GlcNAc_2$ (H5.1) and $Glc_1Man_5GlcNAc_2$ (H6.1). $Glc_1Man_5GlcNAc_2$ was markedly increased, whereas $Man_5GlcNAc_2$ was decreased, when *E. histolytica* trophozoites were labeled in the presence of castanospermine, which is a glucosidase II inhibitor (*inset* in Fig. 2*A*) (30). These results are consistent with the presence of all the components of *N*-glycan-dependent quality control of protein folding in *E. histolytica* (4–6). See supplemental Table 1 for a list of the *E. histolytica* glycosylation-related genes.

When *E. histolytica* membranes were incubated *in vitro* with UDP-[^{3}H]Glc, the most abundant *N*-glycan was also $Glc_1Man_5GlcNAc_2$ (Fig. 6, *B* and *E*). $Glc_1Man_5GlcNAc_2$ was also present in relatively high amounts in mature glycoproteins, indicating that this *N*-glycan is not just a transient species in *E. histolytica* (Fig. 2, *D* and *H*).

Some E. histolytica N-Glycans Are Trimmed Back to $Man_3GlcNAc_2$ and $Man_4GlcNAc_2$ by a Swainsonine-sensitive Mannosidase—The activity of the *E. histolytica* α-mannosidase was inferred by the accumulation of $Man_3GlcNAc_2$

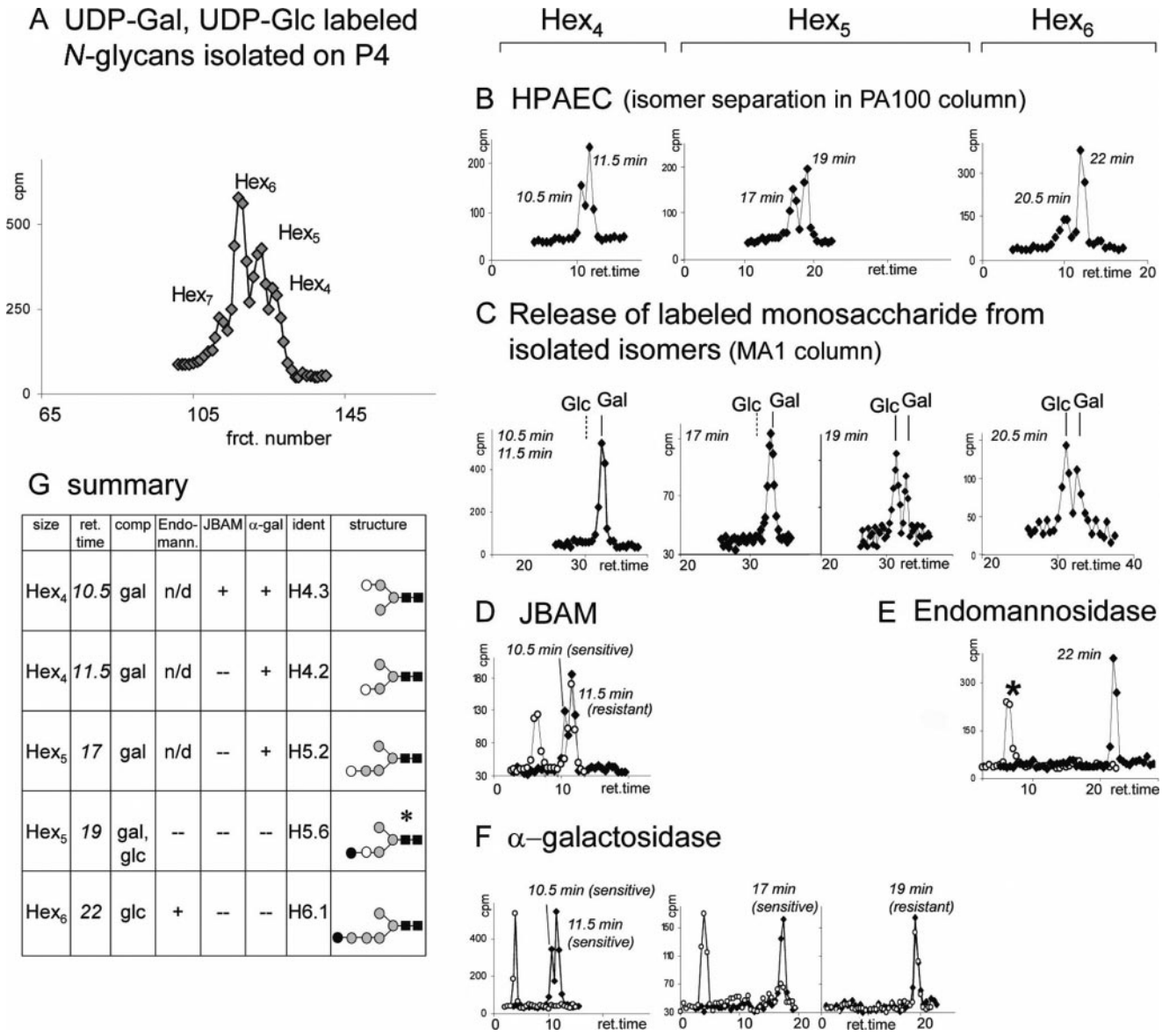

G summary

size	ret. time	comp	Endo-mann.	JBAM	α-gal	ident	structure
Hex_4	*10.5*	gal	n/d	+	+	H4.3	
Hex_4	*11.5*	gal	n/d	--	+	H4.2	
Hex_5	*17*	gal	n/d	--	+	H5.2	
Hex_5	*19*	gal, glc	--	--	--	H5.6	
Hex_6	*22*	glc	+	--	--	H6.1	

FIGURE 6. **Synthesis of complex *N*-glycans *in vitro* by incubating *E. histolytica* membranes with UDP-[^{3}H]Glc and UDP[^{3}H]Gal.** *A*, a Bio-Gel P-4 filtration chromatogram of *N*-glycans is shown. *B*, isomer separation by HPAEC in PA100 is shown. *ret*., retention. *C*, identification of the transferred monosaccharide after total hydrolysis by HPAEC in MA1 is shown. The presence of Gal in the Hex_4 isomers and in Hex_5 eluting at 17 min is consistent with the α-galactosidase digests in *F*. In *D–F*, untreated glycans are marked with *closed circles*, and the products of glycosylhydrolases are marked with *open circles*. *D*, one $Gal_1Man_3GlcNAC_2$ isomer (H4.3, at 10.5 min) is digested with jack bean α-mannosidase (*JBAM*), whereas the other isomer (H4.2, at 11.5 min) is not. *E*, $Glc_1Man_5GlcNAC_2$ (H6.1, at 22 min) is digested to a disaccharide (*asterisk*) by endomannosidase. *F*, both $Gal_1Man_3GlcNAC_2$ isomers (H4.2. and H4.3 at 10.5 and 11.5 min), as well as $Gal_1Man_4GlcNAC_2$ (H5.2 at 17 min), digest with α-galactosidase. In contrast, $Glc_1Gal_1Man_3GlcNAC_2$ (H5.6 at 19 min) is not digested by α-galactosidase. *G*, the table summarizes these results. Isomer H5.2 was fully characterized using complementary data acquired in a separate [2^{3}H]Man-labeling experiment (Fig. 2). *frct*., fraction; *Endomann*, endomannosidase; *comp*, composition; *ident*, identity.

(H3.1) and $Man_4GlcNAc_2$ (H4.1) after labeling *E. histolytica in vivo* for longer times (20–150 min) with [^{3}H]Man (Fig. 2). $Man_4GlcNAc_2$-NYT and $Man_3GlcNAc_2$-NYT were also present after 2–30 min when intact *E. histolytica* membranes were incubated with the OST substrate NYT (Fig. 7) (10, 29, 31). The *E. histolytica* mannosidase activity was inhibited by swainsonine, which has been used previously to inhibit class II mannosidases (Fig. 7) (30). In contrast, the *E. histolytica* mannosidase was not inhibited by deoxymannojirimycin, which inhibits class I mannosidases that are absent from *E. histolytica* (data not shown).

The largest oligosaccharide attached to the radiolabeled tripeptide (NYT) *in vitro* in the presence of UDP-Gal, UDP-Glc, and swainsonine is $Glc_1Man_5GlcNAc_2$ (H6.1) (6). These results suggest that the OST, the mannosidase, and the UDP-Glc:glycoprotein glucosyltransferase are all present in the ER, whereas the Gal- and Glc-transferases (see below) are in a distinct organelle (likely the Golgi apparatus).

Elongation of E. histolytica Complex N-Glycans Is Initiated by Addition of α-Linked Gal to Either Arm of $Man_{3–5}GlcNAc_2$—*E. histolytica* membranes incubated with UDP-[^{3}H]Gal or UDP-[^{3}H]Glc, the two nucleotide sugars that are transported by *E. histolytica* membranes (9), produced abundant products ranging from $Hex_4GlcNAc_2$ (Hex_4) to Hex_7 (Fig. 6). In contrast, radiolabeled products were not formed when *E. histolytica* membranes were incubated with radiolabeled GDP-Man or

GDP-Fuc (data not shown). Indeed, monosaccharide analysis of *N*-glycans of *E. histolytica* labeled *in vivo* with [^{14}C]Glc revealed Man, Gal, and Glc but did not show other hexoses or deoxyhexoses (Fig. 3*B*). Treatment with hexosaminidase, along with mass spectrometry results, showed that *N*-glycan extensions do not contain hexosamines. All of the *N*-glycans of *E. histolytica* were neutral oligosaccharides (data not shown) lacking charged sugars (*e.g.* sialic acids) or other modifications such as sulfation or phosphorylation.

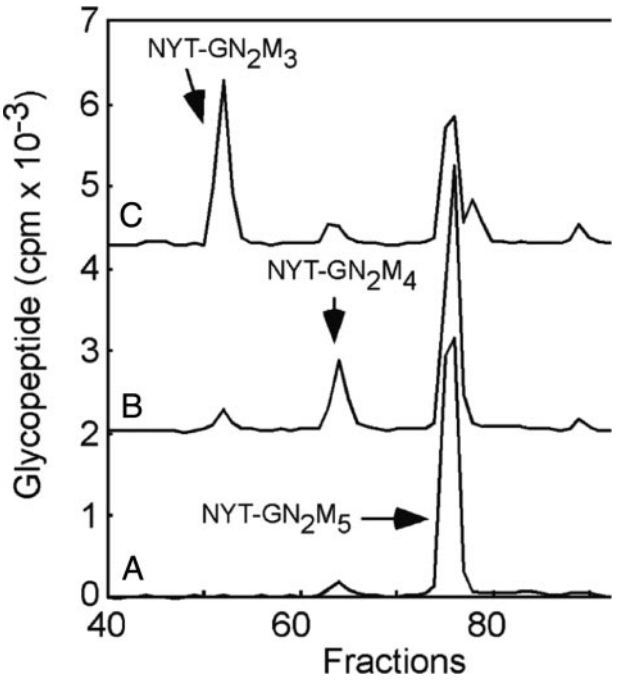

FIGURE 7. ***E. histolytica*** **membranes contain a swainsonine-sensitive** α**-mannosidase.** Glycopeptides produced by incubating intact *E. histolytica* membranes with a radiolabeled tripeptide acceptor (NYT) were captured on concanavalin A and resolved by HPLC. HPLC profiles show glycopeptides from assays incubated in the presence (*A*) or absence (*B* and *C*) of swainsonine for 2 min (*B*) or 30 min (*A* and *C*). Standards include Man$_5$GlcNAc$_2$-NYT, Man$_9$GlcNAc$_2$-NYT, and a glycopeptide mix, Man$_{3-9}$GlcNAc$_2$-NYT.

As shown by sensitivity to α-galactosidase but not to β-galactosidase, a single α-linked Gal was added to the terminal Man on either or both arms of Man$_{2-5}$GlcNAc$_2$ when *E. histolytica* were labeled *in vivo* or *in vitro* (*e.g.* H3.2, H4.2, H4.3, H5.2, H5.4, and H6.4) (Figs. 3 and 4). Fig. 8*B* shows the signature of a terminal 1,2-linked hexose (a $^{1,3}A_2$ fragment that cannot originate from Man$_3$GlcNAc$_2$) (H3.1). This result indicates that the minor Hex$_3$ isomer (H3.2) is indeed elongated with an α1,2-linked Gal. The spectrum for Hex$_6$ *N*-glycans (Fig. 9) also shows the cross-ring $^{1,3}A_2$ fragment, indicating the same Gal configuration (*e.g.* H6.3 to H6.5).

In Many Complex N-Glycans of E. histolytica, Gal Is Capped by One or More Glc Residues—The evidence for complex *E. histolytica N*-glycans containing Gal and Glc included the following. With increasing time, Hex$_7$ to Hex$_{10}$ were present in *N*-glycans of *E. histolytica* labeled *in vivo* with [2-^{3}H]Man (Fig. 2) or [^{14}C]Glc (Fig. 3). As the size of *N*-glycans increased, the percentage of Glc in the oligosaccharides increased (Fig. 3*B*), and these larger *N*-glycans (*e.g.* H5.3, H6.2, H6.5, and H7.1) were resistant to α- and β-galactosidases, consistent with a Glc cap (Fig. 4). With the exception of the product of the UDP-Glc:glycoprotein glucosyltransferase (Glc$_1$Man$_5$GlcNAc$_2$) (H6.1), Glc was only added to *N*-glycans of *E. histolytica* after the addition of Gal (Fig. 6).

Because the complex *N*-glycans of *E. histolytica* that have Glc caps were resistant to all the glycosylhydrolases that we tested, it was not possible to determine whether the Glc- extensions are α- or β-linked; hence, the configuration of the linkage between Glc and Gal remains to be defined. A pseudo MS/MS/MS experiment performed on B_4 ions of Hex$_8$ (which originate from glycans with a linear series of four or more hexoses) suggests the possibility that some of the extending Glc residues are 1,6-linked (supplemental Fig. 4). A full discussion of the mass spectrometry experiments is presented in the supplemental material.

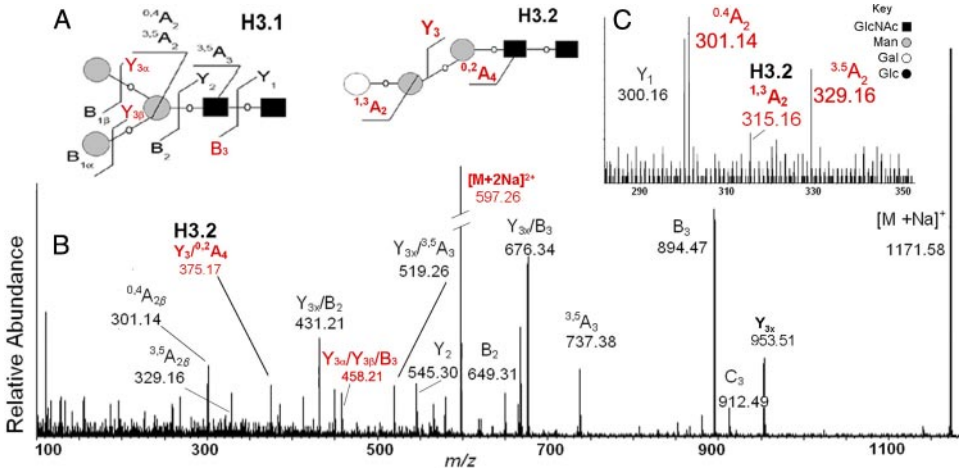

FIGURE 8. **MS^2 collision-induced dissociation spectrum of the Hex$_3$HexNAc$_2$ isolated at *m/z* 597. 33, [M+2Na]$^{2+}$.** *A*, the diagram shows the origin of fragments from the two isomers present in this pool (see Fig. 2*G*). A secondary fragment, $Y_{3\alpha}/Y_{3\beta}/B_3$ at *m/z* 458.21 (*B*), is consistent with archetypal biantennary Man$_3$GlcNAc$_2$. Cross-ring fragments $^{0,4}A_2$, *m/z* 301.14 and $^{3,5}A_2$, *m/z* 329.16 (*C*) define the Manα1,6- arm. A low abundance $^{1,3}A_2$ fragment at *m/z* 315.16 (*C*) indicates the presence of an isomer bearing a terminal 1,2-linked Gal (H3.2). A $Y_3/^{0,2}A_4$ fragment ion seen at *m/z* 375.17 (*B*) is consistent with the core region of a linear isomer. No signal is seen at *m/z* 505.2 or 533.2 (for a substituted Manα1,6-). Therefore, the structure for H3.2 indicates a missing Manα1,6- arm, with the remaining Manα1,3- arm extended with Galα1,2-. These results are consistent with the glycosylhydrolase digestion data (Fig. 4).

DISCUSSION

Properties of E. histolytica N-Glycans That Distinguish Them from N-Glycans of Fungi and Metazoa—As shown by analysis of predicted proteins from whole genome sequences, *E. histolytica* is missing seven asparagine-linked glycosylation enzymes, and so *N*-glycans are built upon the truncated precursor Man$_5$GlcNAc$_2$ (H5.1 in Fig. 1) (see supplemental Table 1) (3). Man$_5$GlcNAc$_2$ is glucosylated by the UDP-Glc:glycoprotein glucosyltransferase of the *N*-glycan-dependent quality control system for protein folding to make Glc$_1$Man$_5$GlcNAc$_2$ (H6.1) (4–6). For the same reason, *N*-gly-

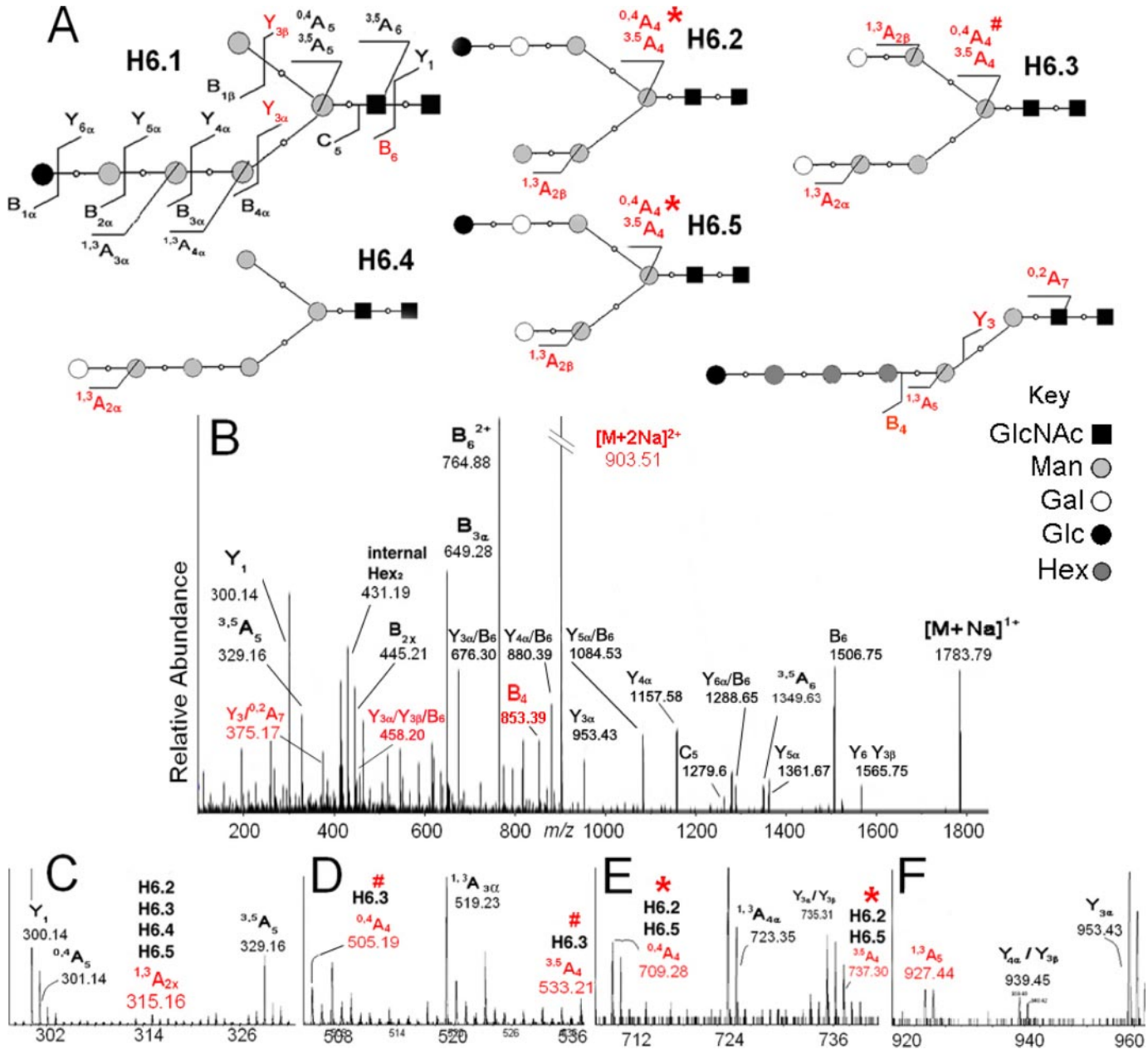

FIGURE 9. **MS^2 collision-induced dissociation spectrum of the $Hex_6GlcNAc_2$ $[M+2Na]^{2+}$ isolated at *m/z* 903. 51.** *A*, the diagram shows the origin of fragments from the isomers present in this pool (see Fig. 2*G*). *Asterisk* and *pound symbols* indicate the origin of cross-ring fragments of the same denomination but different *m/z*. Diagnostic ions for isomers H6.1 and H6.4 are as follows. Fragments $^{0,4}A_5$ and $^{3,5}A_5$, *m/z* 301.14 and 329.16 (*C*) define the unsubstituted Manα1,6- arm, whereas fragment $^{1,3}A_4$, *m/z* 723.35 (*E*) indicates the four hexoses of the Manα1,3- arm. Fragment $Y_{3\alpha}/Y_{3\beta}/B_6$, *m/z* 458.20 (*B*) reveals a biantennary structure. The spectrum supports evidence for Gal extensions. An ion at *m/z* 315.16 (*C*) indicates a $^{1,3}A_{2x}$ fragment. The single isomer predicted to contain terminal Manα1,2- (H6.2) is just ~1% of the pool; therefore, the majority of the $^{1,3}A_{2x}$ fragment originates from the terminal Galα1,2- of the more abundant isomers H6.3, H6.4, and H6.5. Evidence for extensions on the Manα1,6- was found as well. Fragments $^{0,4}A_4$ and $^{3,5}A_4$ at *m/z* 505.19 and 533.21 (*D*) and fragments $^{0,4}A_4$ and $^{3,5}A_4$ at *m/z* 709.28 and 737.30 (*E*) indicate Manα1,6- with one or two hexoses substitutions. Fragment $^{1,3}A_5$ at *m/z* 927.44 (*F*) indicates an α1,2 with a four-hexose extension. These data, together with results from glycosylhydrolase digestions, define isomers H6.3, H6.2, and H6.5.

cans of *T. vaginalis*, the cause of vaginitis, are also built upon $Man_5GlcNAc_2$, which is again glucosylated to $Glc_1Man_5GlcNAc_2$ (3, 6).

In contrast to fungi and metazoa, a large proportion of *E. histolytica N*-glycans reach the plasma membrane as unmodified $Man_5GlcNAc_2$ (H5.1), bypassing ER and Golgi mannosidases and glycosyltransferases. Similarly, a large fraction of mature *N*-glycans of *E. histolytica* are composed of $Glc_1Man_5GlcNAc_2$, as has been described in *Leishmania* (33). The presence of $Glc_1Man_5GlcNAc_2$ in mature glycoproteins suggests that it may have other functions in addition to serving as an intermediate in the *N*-glycan-dependent quality control of folding in the ER lumen (4–6).

Because we did not link *N*-glycans to sites on particular *E. histolytica* glycoproteins, there are three possible explanations for the abundance of unmodified $Man_5GlcNAc_2$ in the plasma membrane. First, *N*-glycans on some *E. histolytica* glycoproteins are never processed. Second, *N*-glycans at multiple sites on the same glycoprotein are processed differently. Third, *E. histolytica* mannosidases and glycosyltransferases that make

complex *N*-glycans are very inefficient. We speculate that the high Man *N*-glycans of *E. histolytica* may be harder to recognize by the host immune system than the unique complex *N*-glycans of *E. histolytica*. A similar argument has been made to explain the abundance of high Man *N*-glycans on gp120 of HIV (14).

The capping of *E. histolytica* plasma membrane glycoproteins containing $Man_5GlcNAc_2$ by cyanovirin-N suggests the possibility that anti-viral lectins such as cyanovirin-N might be used to block binding of *E. histolytica* to the host epithelium. Cyanovirin-N inhibits phagocytosis of mucin-coated beads by *E. histolytica*.[3] As well, affinity columns with concanavalin A efficiently capture *E. histolytica* glycoproteins with *N*-glycans (so-called *N*-glycome) for mass spectrometric identification of peptides.[3]

In addition to OST and UDP-Glc:glycoprotein glucosyltransferase activities (6, 8), the ER of *E. histolytica* contains a swainsonine-inhibitable α-mannosidase, which trims a fraction of the *N*-glycans to $Man_3GlcNAc_2$ (H3.1) and $Man_4GlcNAc_2$ (H4.1). As in metazoa, the trimmed *N*-glycans of *E. histolytica* are building blocks for formation of complex *N*-glycans (34, 35).

E. histolytica has a single predicted α-mannosidase (glycosylhydrolase family 92 or GH92), which is similar to those of some fungi (*Aspergillus*, *Neurospora*, and *Magnaporta*) and many Gram-positive bacteria (*e.g. Streptococcus*, *Porphyromonas*, *Bacteroides*, and *Mycobacteria*) (supplemental Table 1) (20–22). Phylogenetic analyses strongly suggest that the *E. histolytica* GH92 mannosidase was obtained by lateral gene transfer because the *E. histolytica* mannosidase is present in a clade with bacteria, and this clade is supported with high bootstrap values (supplemental Fig. 5). In contrast, the fungal mannosidases were present in clades that did not include the *E. histolytica* mannosidase. Lateral gene transfer is an important mechanism by which *E. histolytica* has obtained many dozen bacterial genes encoding fermentation and other enzymes (20). *E. histolytica* is missing mannosidases similar to ER or Golgi mannosidases (GH47) or to lysosomal mannosidases (GH38) (20–22, 32).

The *N*-glycans of *E. histolytica*, which have α1,2-linked Gal that is extended with Glc, are simpler than the complex *N*-glycans of metazoa. The *N*-glycans of *E. histolytica* are consistent with the experimental demonstration of two *E. histolytica* nucleotide sugar transporters (for UDP-Glc and UDP-Gal) (9) and with bioinformatic predictions of a limited number of Golgi glycosyltransferases in *E. histolytica* (see supplemental Table 1). *O*-phosphodiester-linked glycans of *E. histolytica* are also composed of Gal capped with Glc, but the linkages are different from those of *N*-glycans (10). Although α1,2-Gal linked to Man is also present in *N*-glycans of *Schizosaccharomyces pombe* (36), *N*-glycans with distal Glc capping residues are not present in the human host of *E. histolytica*. This suggests the possibility that the unique complex *N*-glycans of *E. histolytica* may be targets for future anti-amebic vaccines. In support of this idea, the *O*-phosphodiester-linked glycans, which are also rich in Gal and Glc, are one of a limited number of current anti-amebic vaccine targets (1, 2, 10).

[3] D. Ratner and J. Samuelson, unpublished observations.

REFERENCES

1. Haque, R., Huston, C. D., Hughes, M., Houpt, E., and Petri, W. A., Jr. (2003) *N. Engl. J. Med.* **348,** 1565–1573
2. Stanley, S. L. (2003) *Lancet* **361,** 1025–1034
3. Samuelson, J., Banerjee, S., Magnelli, P., Cui, J., Kelleher, D. J., Gilmore, R., and Robbins, P. W. (2005) *Proc. Natl. Acad. Sci. U. S. A.* **102,** 1548–1553
4. Helenius, A., and Aebi, M. (2004) *Annu. Rev. Biochem.* **73,** 1019–1049
5. Trombetta, E. S., and Parodi, A. J. (2003) *Annu. Rev. Cell Dev. Biol.* **19,** 649–676
6. Banerjee, S., Vishwanath, P., Cui, J., Kelleher, D. J., Gilmore, R., Robbins, P. W., and Samuelson, J. (2007) *Proc. Natl. Acad. Sci. U. S. A.* **104,** 11676–11681
7. Kelleher, D. J., and Gilmore, R. (2006) *Glycobiology* **16,** 47R–62R
8. Kelleher, D. J., Banerjee, S., Cura, A. J., Samuelson, J., and Gilmore, R. (2007) *J. Cell Biol.* **177,** 29–37
9. Bredeston, L. M., Caffaro, C. E., Samuelson, J., and Hirschberg, C. B. (2005) *J. Biol. Chem.* **280,** 32168–32176
10. Moody-Haupt, S., Patterson, J. H., Mirelman, D., and McConville, M. J. (2000) *J. Mol. Biol.* **297,** 409–420
11. Petri, W. A., Jr., Haque, R., and Mann, B. J. (2002) *Annu. Rev. Microbiol.* **56,** 39–64
12. Adler, P., Wood, S. J., Lee, Y. C., Lee, R. T., Petri, W. A., Jr., and Schnaar, R. L. (1995) *J. Biol. Chem.* **270,** 5164–5171
13. Arhets, P., Gounon, P., Sansonetti, P., and Guillen, N. (1995) *Infect. Immun.* **63,** 4358–4367
14. Kwong, P. D., Doyle, M. L., Casper, D. J., Cicala, C., Leavitt, S. A., Majeed, S., Steenbeke, T. D., Venturi, M., Chaiken, I., Fung, M., Katinger, H., Parren, P. W., Robinson, J., Van Ryk, D., and Wang, L. (2002) *Nature* **420,** 678–682
15. Adams, E. W., Ratner, D. M., Bokesch, H. R., McMahon, J. B., O'Keefe, B. R., and Seeberger, P. H. (2004) *Chem. Biol.* **11,** 875–881
16. Scanlan, C. N., Pantophlet, R., Wormald, M. R., Ollmann Saphire, E., Stanfield, R., Wilson, I. A., Katinger, H., Dwek, R. A., Rudd, P. M., and Burton, D. R. (2002) *J. Virol.* **76,** 7306–7321
17. Barboza, M., Duschak, V. G., Fukuyama, Y., Nonami, H., Erra-Balsells, R., Cazzulo, J. J., and Couto, A. S. (2005) *FEBS J.* **272,** 3803–3815
18. Atrih, A., Richardson, J. M., Prescott, A. R., and Ferguson, M. A. (2005) *J. Biol. Chem.* **280,** 865–871
19. Guha-Niyogi, A., Sullivan, D. R., and Turco, S. J. (2001) *Glycobiology* **11,** 45R–59R
20. Loftus, B., Anderson, I., Davies, R., Alsmark, U. C., Samuelson, J., Amedeo, P., Roncaglia, P., Berriman, M., Hirt, R. P., Mann, B. J., Nozaki, T., Suh, B., Pop, M., Duchene, M., and Ackers, J. (2005) *Nature* **433,** 865–868
21. Altschul, S. F., Madden, T. L., Schaffer, A. A., Zhang, J., Zhang, Z., Miller, W., and Lipman, D. J. (1997) *Nucleic Acids Res.* **25,** 3389–3402
22. Coutinho, P. M., Deleury, E., Davies, G. J., and Henrissat, B. (2003) *J. Mol. Biol.* **328,** 307–317
23. Krogh, A., Larsson, B., von Heijne, G., and Sonnhammer, E. L. (2001) *J. Mol. Biol.* **305,** 567–580
24. Nielsen, H., Brunak, S., and von Heijne, G. (1999) *Protein Eng.* **12,** 3–9
25. Lubas, W. A., and Spiro, R. G. (1987) *J. Biol. Chem.* **262,** 3775–3781
26. Clark, C. G., and Diamond, L. S. (2002) *Clin. Microbiol. Rev.* **15,** 329–341
27. Ciucanu, I., and Kerek, F. (1984) *Carbohydr. Res.* **131,** 209–217
28. Domon, B., and Costello, C. E. (1998) *Biochemistry* **27,** 1534–1543
29. Kelleher, D. J., Kreibich, G., and Gilmore, R. (1992) *Cell* **69,** 55–65
30. Elbein, A. D. (1991) *FASEB J.* **5,** 3055–3063
31. Kelleher, D. J., Karaoglu, D., and Gilmore, R. (2001) *Glycobiology* **11,** 321–333
32. Herscovics, A. (1999) *Biochim. Biophys. Acta* **1473,** 96–107
33. Funk, V. A., Thomas-Oates, J. E., Kielland, S. L., Bates, P. A., and Olafson, R. W. (1997) *Mol. Biochem. Parasitol.* **84,** 33–48
34. Betenbaugh, M. J., Tomiya, N., Narang, S., Hsu, J. T., and Lee, Y. C. (2004) *Curr. Opin. Struct. Biol.* **14,** 601–606
35. Lowe, J. B., and Marth, J. D. (2003) *Annu. Rev. Biochem.* **72,** 643–691
36. Chappell, T. G., Hajibagheri, M. A., Ayscough, K., Pierce, M., and Warren, G. (1994) *Mol. Biol. Cell* **5,** 519–528
37. Yamashita, K., Tachibana, Y., Nakayama, T., Kitamura, M., Endo, Y., and Kobata, A. (1980) *J. Biol. Chem.* **255,** 5635–5642